



## Article

# Technical Feasibility and Histological Analysis of Balloon-Expandable Metallic Stent Placement in a Porcine Eustachian Tube

Yehree Kim <sup>1,†</sup>, Woo Seok Kang <sup>1,†</sup>, Jeon Min Kang <sup>2</sup>, Dae Sung Ryu <sup>2</sup>, Min Young Kwak <sup>3</sup> , Ho-Young Song <sup>4</sup>, Jung-Hoon Park <sup>2,\*,‡</sup>  and Hong Ju Park <sup>2,\*,‡</sup>

<sup>1</sup> Asan Medical Center, Departments of Otorhinolaryngology-Head & Neck Surgery, College of Medicine, University of Ulsan, 88 Olympic-ro 43-gil, Songpa-gu, Seoul 05505, Korea; yehreek@wmail.ulsan.ac.kr (Y.K.); wooseok\_kang@amc.seoul.kr (W.S.K.)

<sup>2</sup> Biomedical Engineering Research Center, Asan Institute for Life Sciences, Asan Medical Center, 88 Olympic-ro 43-gil, Songpa-gu, Seoul 05505, Korea; miny2208@amc.seoul.kr (J.M.K.); kryuds@amc.seoul.kr (D.S.R.)

<sup>3</sup> Department of Otolaryngology-Head and Neck Surgery, College of Medicine, Eulji University, Daejeon 35233, Korea; 20201006@eulji.ac.kr

<sup>4</sup> Department of Radiology, University of Texas Health Science Center at San Antonio, 7703 Floyd Curl Drive, San Antonio, TX 78229, USA; hysong@amc.seoul.kr

\* Correspondence: jhparkz@amc.seoul.kr (J.-H.P.); dzness@amc.seoul.kr (H.J.P.)

† Y.K. and W.S.K. contributed equally to this work and are the co-first authors.

‡ J.-H.P. and H.J.P. contributed equally to this work and are the co-corresponding authors.



**Citation:** Kim, Y.; Kang, W.S.; Kang, J.M.; Ryu, D.S.; Kwak, M.Y.; Song, H.-Y.; Park, J.-H.; Park, H.J. Technical Feasibility and Histological Analysis of Balloon-Expandable Metallic Stent Placement in a Porcine Eustachian Tube. *Appl. Sci.* **2021**, *11*, 1359. <https://doi.org/10.3390/app11041359>

Academic Editor: Akram Alomainy  
Received: 16 January 2021  
Accepted: 2 February 2021  
Published: 3 February 2021

**Publisher's Note:** MDPI stays neutral with regard to jurisdictional claims in published maps and institutional affiliations.



**Copyright:** © 2021 by the authors. Licensee MDPI, Basel, Switzerland. This article is an open access article distributed under the terms and conditions of the Creative Commons Attribution (CC BY) license (<https://creativecommons.org/licenses/by/4.0/>).

**Abstract:** There is a clinical need to develop a stent to treat obstructive and refractory Eustachian tube dysfunction (ETD) after balloon Eustachian tuboplasty. An animal model for stent placement in the Eustachian tube (ET) is needed to develop optimal designs and materials, as stents for ETD have not been clinically applied. The purpose of this study was to evaluate the technical feasibility of stent placement and histological changes in a porcine ET model. Six ETs were evaluated in three pigs. Cobalt–chrome alloy stents with two different diameters were placed in the left and right ET of each animal (right, 3.5 mm; left, 2.5 mm). The outcomes were assessed by endoscopic and fluoroscopic imaging during the procedure, computed tomography after the procedure, and by histological examinations. Stent placement was technically successful in all specimens after metallic guiding sheaths were located in the nasopharyngeal end of the ET. The mean luminal diameters of the proximal, middle, and distal portions of the larger stents in the right ETs were 3.48 mm, 2.54 mm, and 2.15 mm, respectively. In the left ETs using smaller stents, these values were 2.49 mm, 1.73 mm, and 1.42 mm, respectively. The diameters of the inserted stents differed by stent location and the original diameter. Histological findings showed tissue hyperplasia with severe inflammatory cell infiltration at 4 weeks after stent placement. In conclusion, stent placement into the porcine ET was technically feasible, and stent-induced tissue hyperplasia was significantly evident. The luminal configuration of the placed ET stent changed according to its non-elastic nature and anatomical features of the porcine ET. Using this model, ET stents of various materials and designs with anti-inflammatory or anti-proliferative drugs can be optimized for future treatments of ET dysfunction.

**Keywords:** Eustachian tube; stent; Eustachian tube dysfunction; tissue hyperplasia; otitis media

## 1. Introduction

The Eustachian tube (ET) forms the only connection between the middle ear and the nasopharynx; thus, its normal function is important for maintaining a healthy, well-aerated middle ear [1]. The functions of the ET include secretion transport, middle ear ventilation, and protection against pathogens and nasopharyngeal reflux [2]. Dysfunction of the ET can lead to the development of acute and chronic otitis media, one of the most common disorders encountered in otolaryngology practice [3].

Until recently, otolaryngologists' understanding of ET dysfunction (ETD) was limited and few treatment options were available [4–8]. Currently, the most common surgical approach is myringotomy with or without the insertion of a ventilation tube, with a reported success rate of 79% after a 4-month follow-up period [6]. However, this is only a temporary management solution and it does not address the ET directly. Other conservative management solutions for ETD also include the Valsalva maneuver for pressure equalization and use of nasal steroids and decongestants [9]. With the introduction of balloon Eustachian tuboplasty (BET), however, surgical management of ETD is now possible [10]. The proposed mechanisms underlying the effects of BET include microtears in the cartilaginous part of the ET [10], decreased mucosal inflammation, and reduced biofilm infection load [11]. Since 2010, studies have reported the use of BET to treat ETD, with success rates ranging between 36% and 80% [8,12–14]. Although these prior studies reported that BET is superior to conventional medical management, some patients with ETD do not respond to this dilation treatment.

The possible options for the further management of patients with BET failure include a repeat BET procedure or the insertion of an ET stent [15]. However, stents for ETD have not been clinically applied. Thus, animal studies are needed to develop a stent option for ETD and to compare histologic changes in the ET after a repeat BET or insertion of an ET stent. The current study established a porcine model for ET stenting and validated the feasibility of inserting commercially available stents of two different diameters using combined endoscopic and fluoroscopic guidance. This study aimed to investigate the technical feasibility of stent placement and histological changes after stent placement in a porcine ET and evaluate the optimal size and luminal configuration of ET stents for the porcine model.

## 2. Materials and Methods

### 2.1. Study Design

This study tested both ETs in three pigs weighing 33.7, 37.2, and 35.4 kg, respectively (i.e., six total ETs). The technical feasibility of stent placement in a porcine ET was assessed by fluoroscopic and endoscopic images obtained during the procedure and computed tomography (CT) afterward. The stent sizes were selected according to the diameter (2.3 to 3.4 mm) and length (24.2 to 36.4 mm) of the normal ET in a porcine model [15,16]. This study was approved by the Institutional Animal Care and Use Committee of the Asan Institute for Life Sciences (2020-12-189) and conformed to US National Institutes of Health guidelines for humane handling of laboratory animals.

### 2.2. Metallic Guiding Sheath

A newly developed metallic guiding sheath for use in the porcine ET model was fabricated from stainless steel (Genoss Co., Ltd., Suwon, Korea; Figure 1a).

This sheath had inner and outer diameters of 2 and 2.5 mm, respectively, and was 250 mm long. The distal 20 mm of the sheath was curved into a J shape at a 30° angle to the axis to enable easy access from the nose to the nasopharyngeal orifice of the ET in the pigs. The angled distal tip of the sheath was easily located in the nasopharyngeal orifice of the ET.

### 2.3. Stent Placement under Endoscopic and Fluoroscopic Guidance

Anesthesia was induced by intramuscular injection of 50 mg of ketamine under the supervision of a veterinarian. An endotracheal tube was placed and anesthesia was maintained by inhalation (0.5–2% isoflurane (Ifiran; Hana Pharm. Co., Seoul, Korea) with oxygen (510 mL/kg per min) at 1:1). The pigs were then positioned in the prone position and baseline endoscopic images of the nasopharyngeal orifice of the ET were obtained. The metallic guiding sheath (arrowheads, Figure 1a) was then advanced through the nostril to the nasopharyngeal orifice (arrow, Figure 1a) of the ET under endoscopic guidance (Figure 1). A micro-guidewire with a balloon catheter (Genoss Co., Ltd., Suwon, Korea), which had been

crimped with a stent, was then advanced through the metallic guiding sheath (arrowheads, Figure 1c) into the ET until its tip met resistance near the bony-cartilaginous isthmus of the ET. This procedure was conducted under combined endoscopic (VISERA 4K UHD Rhinolaryngoscope; Olympus, Tokyo, Japan; arrows, Figure 1e) and fluoroscopic (Ziehm Vision RFD Hybrid Edition; Ziehm Imaging GmbH, Nuremberg, Germany) guidance. Cobalt-chrome alloy stents of two different diameters (18 mm length and 85  $\mu$ m strut thickness, Genoss BMS, Genoss Co., Ltd., Suwon, Korea) were then placed into the left and right ETs (right-side ET, 3.5 mm; left-side ET, 2.5 mm). The balloon catheter was fully inflated with a contrast medium to 12 atmospheres, as determined by a pressure gauge monitor. After maintaining the fully expanded balloon for 30 seconds, the balloon catheter was deflated under continuous fluoroscopic monitoring. The sheath, balloon catheter, and guidewire were removed after stent placement and the ET orifice was examined by endoscopy to confirm the location of the proximal end of the stent and detect any mucosal injuries. Technical success was defined as successful stent placement in the cartilaginous portion of the porcine ET. All pigs were euthanized using an overdose of xylazine hydrochloride (Rompun; Bayer, Seoul, Korea) at 4 weeks after stent placement. Before sacrifice, follow-up endoscopic examinations were performed to evaluate the proximal end of the stent.

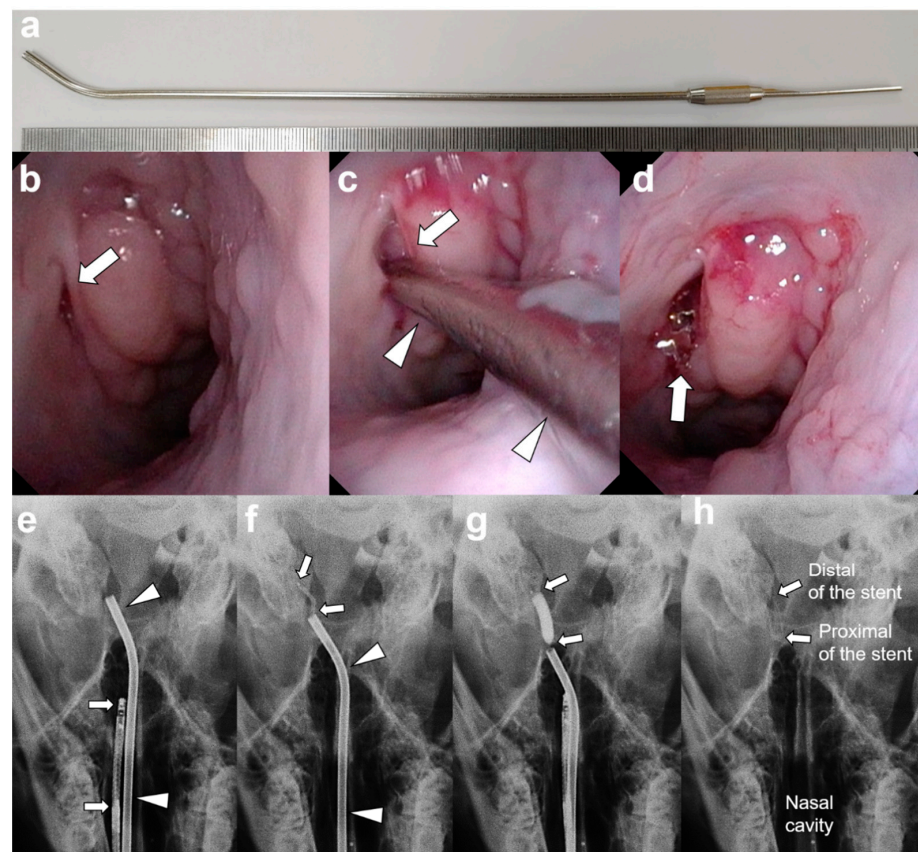


**Figure 1.** (a) Photograph showing the metallic guiding sheath developed for the porcine Eustachian tube (ET) model. (b–h) The technical steps of stent placement in a porcine ET. (b) Baseline endoscopic image showing the nasopharyngeal orifice (arrow) of the right ET. (c) Endoscopic image showing the location of the metallic guiding sheath (arrowheads) at the ET orifice. (d) The proximal end of the stent (arrow) protrudes from the nasopharyngeal orifice of the ET. (e) Radiograph obtained during stent placement showing the metallic guiding sheath (arrowheads) and flexible endoscopy (arrows). (f) A balloon catheter with a crimped stent (arrows) was inserted through the sheath (arrowheads) into the ET. (g) The balloon catheter (arrows) was fully inflated. (h) Radiograph obtained immediately after stent placement showing a fully expanded stent (arrows).

#### 2.4. Computed Tomography

Images of the temporal bones were obtained by CT (Somatom Sensation 16; Siemens, Erlangen, Germany) performed immediately after stent placement to verify the stent location and patency, and to measure the inner luminal diameters of the stent at the proximal, middle, and distal portions of the ET.

#### 2.5. Gross and Histological Examination

Surgical exploration of the ET with the placed stent was followed by gross examination to detect tissue injuries occurring during stent placement and to observe the status of the placed stent. For this analysis, the cadaveric porcine heads were mid-sagittally sectioned using an electric saw. The stent was then carefully extracted for histological examination. The ET tissue samples were fixed in 10% neutral-buffered formalin for 24 h. The fixed tissue samples were then embedded in plastic resins and axially sectioned at the segment with the stent. The slides were stained with hematoxylin and eosin. Histologic analysis was performed using a digital slide scanner (Pannoramic 250 FLASH III, 3D HISTECH Ltd., Budapest, Hungary). Measurements were obtained with a digital microscope viewer (CaseViewer, 3D HISTECH Ltd.).

#### 2.6. Statistical Analysis

Data are expressed as the means  $\pm$  standard deviation (SD). The differences between the two specimens were analyzed using Mann–Whitney U tests. Here,  $p$ -values  $< 0.05$  were considered statistically significant. Statistical analyses were performed using IBM SPSS Statistics for Windows version 24.0 (IBM Corp., Armonk, NY, USA).

### 3. Results

None of the pigs showed any anatomical variations, ear injuries, or disease on pre-procedural endoscopic examinations. The stent placements were technically successful in all pigs, with no procedure-related complications. Although mucosal injuries with touch bleeding were observed in two (33.3%) of the six specimens during sheath insertion, all metallic guiding sheaths were successfully located in the nasopharyngeal orifice of the ET under endoscopic guidance.

In the right-side ETs treated with the larger 3.5-mm-diameter stents, the proximal ends of the stents protruded from the orifice by approximately 1–2 mm. In the left-side ETs, two of the three smaller 2.5-mm-diameter stents were located within the cartilaginous portion of the ET, while one stent was located in the cartilaginous portion of the ET with the proximal tip slightly protruding into the nasopharyngeal orifice of the ET. The longest luminal diameters at the three different stent levels and the decrease rates at each site are presented in Table 1 and Figure 2, with representative examples shown in Figure 3.

**Table 1.** Mean luminal diameters and decrease rates at the proximal, middle, and distal portions of the placed stents in a porcine Eustachian tube (ET) model.

Stent Diameter/Site	Location	Luminal Diameter (mm)	Decrease Rate (%)
3.5 mm/Right ET	Proximal	3.48 $\pm$ 0.06	0.9 $\pm$ 0.8
	Middle	2.54 $\pm$ 0.17	27.4 $\pm$ 7.6
	Distal	2.15 $\pm$ 0.14	38.6 $\pm$ 4.1
2.5 mm/Left ET	Proximal	2.49 $\pm$ 0.04	0.4 $\pm$ 0.6
	Middle	1.73 $\pm$ 0.21	30.8 $\pm$ 8.3
	Distal	1.42 $\pm$ 0.18	43.2 $\pm$ 7.1

Note. Data are means  $\pm$  standard deviation.

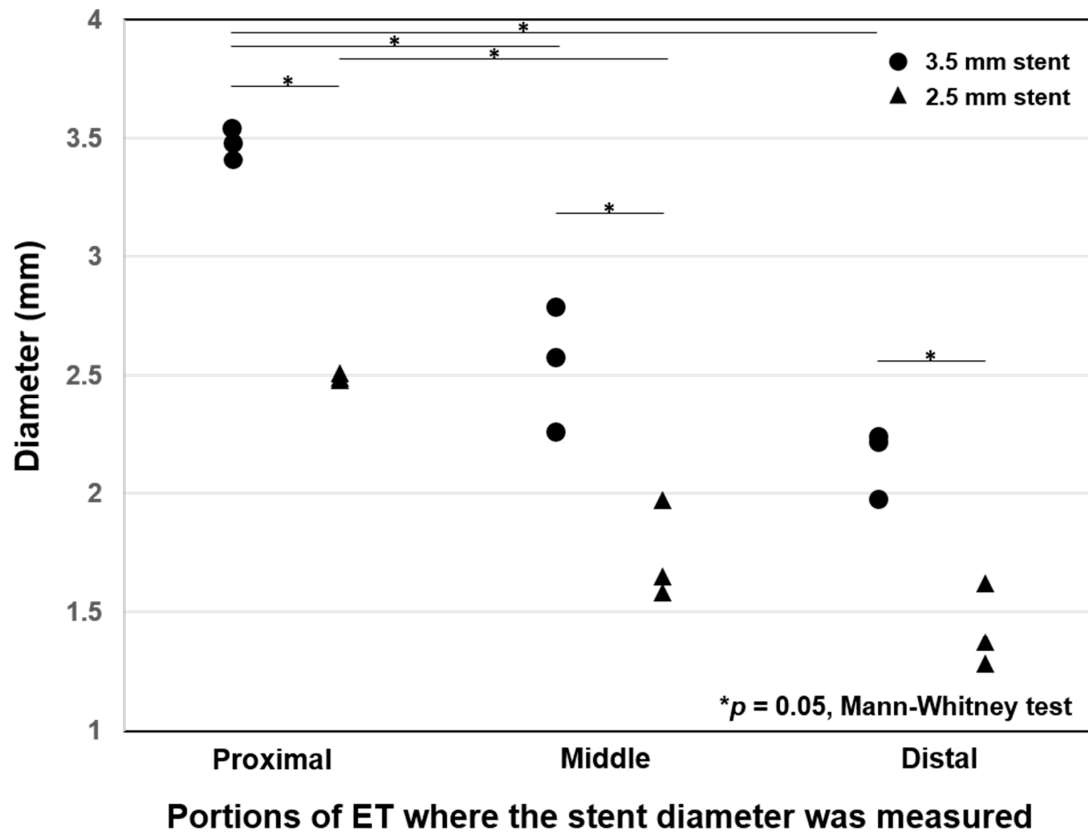


**Figure 2.** Longest luminal diameter of the stent measured at the proximal, middle, and distal portions of the porcine Eustachian tube (ET) model.

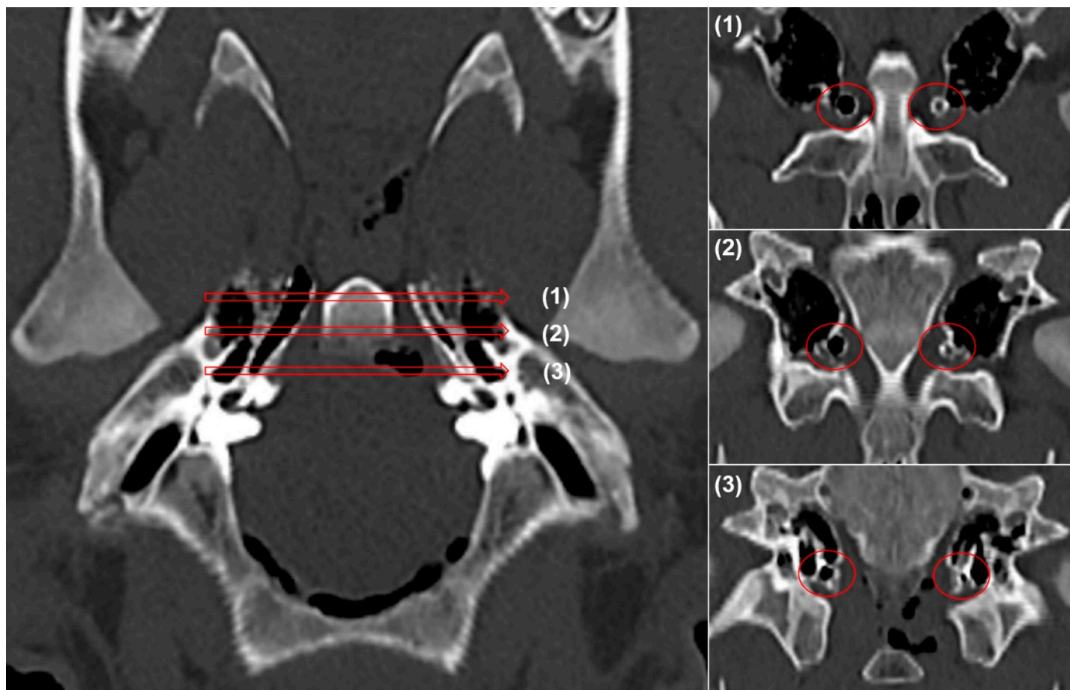


**Figure 3.** Coronal computed tomography image showing segments of the stented ETs, where the stents were present in the (1) proximal, (2) middle, and (3) distal portions. The axial CT images of the proximal portions of the stents show fully expanded stents in both ETs (red circles). The axial CT images show a gradual decrease from the proximal to the distal portion of the stented ET.

The mean luminal diameters ( $\pm$ SD) of the proximal, middle, and distal portions of the stents in the right-side ETs using larger-diameter (3.5 mm) stents were  $3.48 \pm 0.06$ ,  $2.54 \pm 0.17$ , and  $2.15 \pm 0.14$  mm, respectively. In the left-side ETs using smaller-diameter (2.5 mm) stents, these values were  $2.49 \pm 0.04$ ,  $1.73 \pm 0.21$ , and  $1.42 \pm 0.18$  mm, respectively. The diameters of the inserted stents differed significantly by stent location and original diameter.

The excised specimens with the placed stent showed no mucosal injuries in the ETs. The distal portions of the stents were severely collapsed in gross observation of the inserted stents (Figure 4). The stents gradually collapsed from the proximal to the distal portions. The shapes of the inserted stents were influenced by the stent sizes and anatomic configuration of the ET.

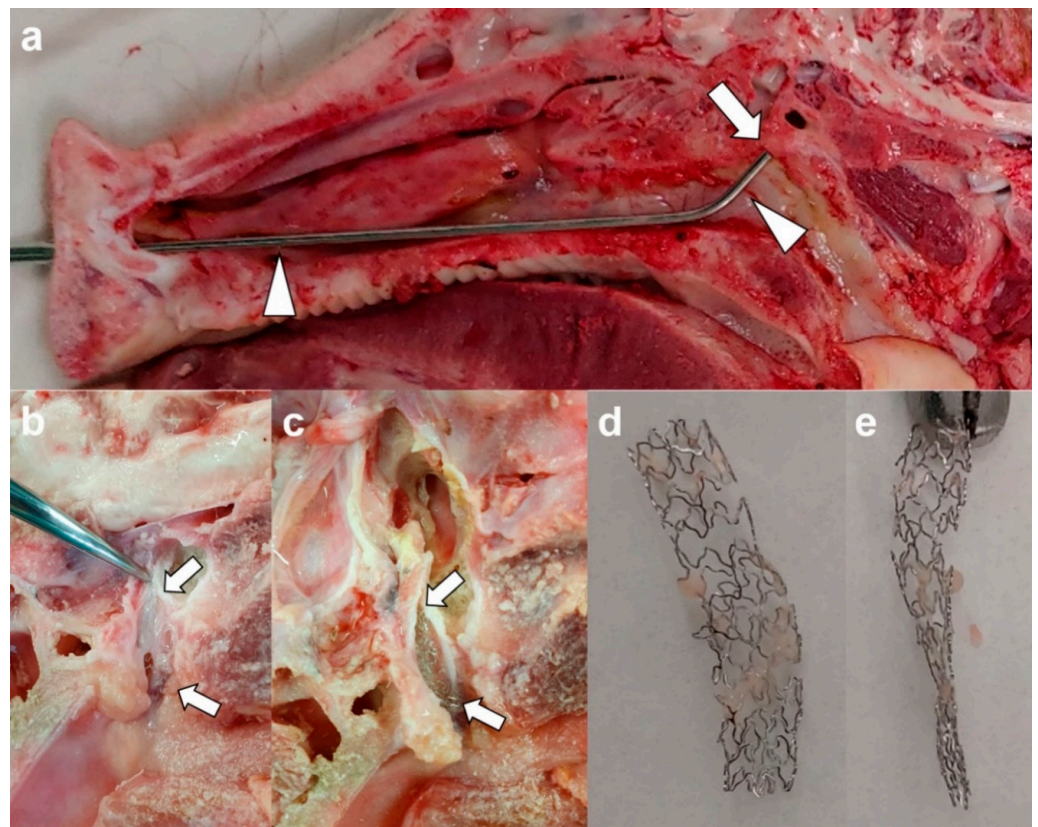


**Figure 4.** (a) Photograph showing a mid-sagittal sectioned cadaveric porcine head with the metallic guiding sheath (arrowheads) facing the orifice of the ET (arrow). (b,c) The photographs show the placed stent (arrows) in the ET and the extracted stent from the ET of the (d) frontal and (e) lateral views. The stent was gradually collapsed from the proximal to the distal portion.

The histological images showed severe inflammatory cell infiltration around the stent strut. Tissue hyperplasia with increased submucosal fibrosis progressed through the stent strut (Figure 5a–c). Follow-up endoscopic images demonstrated that stent migration did not occur at 4 weeks after stent placement. However, the proximal end of the stent was filled with secretion (Figure 5d).

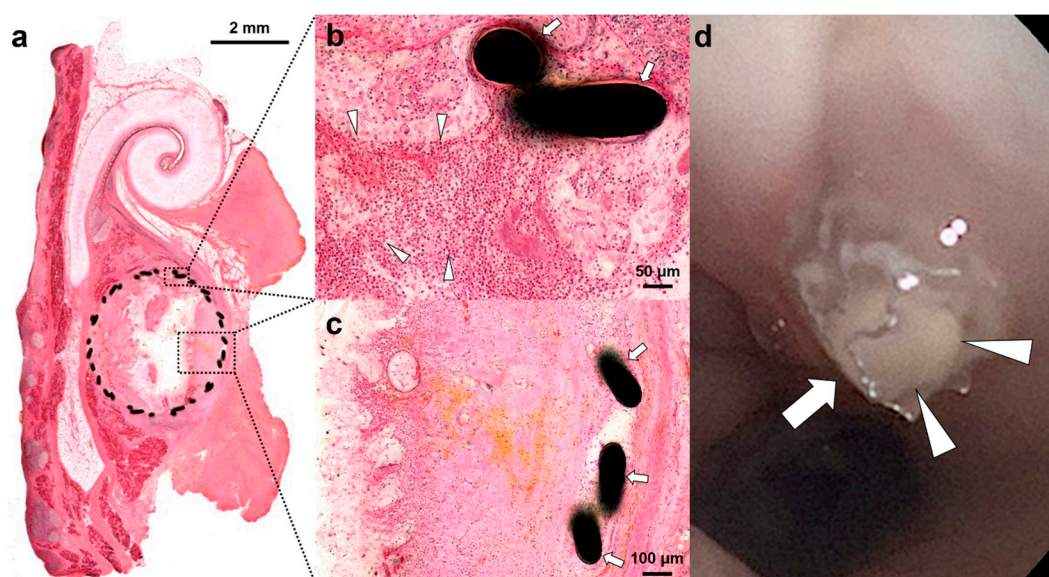


**Figure 5.** Representative histologic (hematoxylin and eosin staining at 1.25 $\times$  (a), 20 $\times$  (b), and 10 $\times$  (c)) and endoscopic images at 4 weeks after stent placement. (a) Microscopic image of a histologic section. (b) Severe inflammatory cell infiltration (arrowheads) adjacent to the stent strut (arrows). (c) Tissue hyperplasia with increased submucosal fibrosis through the stent strut (arrows). (d) Follow-up endoscopic image obtained 4 weeks after stent placement showing the stent (arrows) in place and the proximal end of the stent filled with secretion (arrowheads).

#### 4. Discussion

The primary aim of our present study was to test the feasibility of stent insertion into the ET from the nasopharynx under endoscopic guidance in a porcine model. We inserted commercially available metallic stents with endoscopic guidance and subsequently validated their successful placement using fluoroscopy, CT scans, and necropsy.

The introduction of BET interventions allowed the surgical management of an obstructive ETD. Since 2010, studies have reported the use of BET in ETD, with success rates of 36%–80% [8,10,12,13,17]. Although these prior studies all reported that BET was superior to conventional medical management, this dilation treatment was not successful in some cases, necessitating a further management option. Stents are commonly used for the treatment of obstructive disorders in many non-vascular systems, such as the digestive, respiratory, and urinary tracts [18–20]. However, there have been no attempts to use stents for the treatment of obstructive ETD and side effects have been reported for stent insertions into the non-vascular luminal organs. The development of new strictures due to stent-induced tissue hyperplasia caused by mechanical injuries remains a significant obstacle to successful stent placement in non-vascular luminal organs [18–21]. Another cause of stent re-obstruction is biofilm formation with infections on the stent surfaces [22–24]. Our histological results also demonstrated severe tissue hyperplasia through the stent strut in the porcine ET at 4 weeks after stent placement. Various functional stents, such as drug-eluting biodegradable or non-biodegradable and nano-functionalized stents using gold or silver nanoparticles, have been investigated using various stented animal models to overcome these problems [25–28]; however, therapeutic strategies for the treatment of obstructive ETD that could be tested in human clinical trials have yet to be developed. Various stented animal models have been introduced to study the mechanisms of stent-induced stricture formation [25–30]. Herein, we introduced a well-established ET porcine model to study the mechanisms of complications of stent insertion for ETD and developed a system to reliably test stent materials and configurations.

We utilized cobalt–chrome alloy stents in our current analysis to test the technical feasibility of inserting a stent into the ET. The stent materials that have been used for the treatment of obstructive disorders in other systems include stainless steel, cobalt–chrome

alloy, nitinol wire, and biodegradable substances [31–33]. The ideal stent material should be biocompatible and radiopaque, relieve symptoms caused by obstructive disorders, have low foreign body sensation, not induce susceptibility to infection, and be available at a reasonable cost. The cobalt–chrome tested in the present study was readily available because it is commonly used in coronary arterial disease [34]. However, this material has some disadvantages, including a lack of MRI compatibility, poor fluoroscopic visibility, and non-elastic force [35]. Stents made from nitinol, a shape memory alloy with super-elastic properties, are commonly used to treat obstructive disorders in non-vascular systems, such as those of the digestive, respiratory, and urinary systems [18–20]. The ideal material for ET stents has not yet been determined and further studies are needed on this topic in animal ET models.

In the present study, the diameters of the inserted stents differed significantly by the location and original diameter of the stent (Figure 2). The distal ends of the stents were collapsed due to the non-elastic force of the cobalt–chrome, as well as the anatomical structure of the ET. This finding suggested that the shape of the ET stent needed to be configured based on the anatomical structure of the cartilaginous ET. The shape of the inserted stents may also conceivably be altered by movements surrounding the ET in a living animal, such as swallowing and chewing. Additional long-term, post-insertion observation studies are needed to identify an ideal configuration for ET stents.

Generally, sheep and pigs are considered good models of the human middle ear [36]. A previous study of ET stent insertion conducted in a sheep model suggested that as the pig's ET consists of a cartilaginous structure, the sheep ET was more anatomically similar to the human ET. However, the stent should be placed in the cartilaginous portion of the ET and the primary purpose of an animal model for testing an ET stent is to identify the optimal materials and shape of the stent that results in minimal complications. We contend that this can be readily achieved by investigating the histologic changes to the cartilaginous ET in pigs, thus making our model useful.

This study had several limitations. First, the total number of specimens was relatively small to perform a robust statistical analysis. Second was the lack of a control group, namely non-treated animals, because of the limited number of animals. Additional studies are required for comparison with an untreated control group in the porcine ET and to evaluate the histological changes and tissue reaction after stent placement with long-term follow-up. Furthermore, stent modification according to the length and shape of the ET should be considered based on our findings; moreover, the application of drug-eluting stents in the ET should be considered to prevent inflammatory reaction and stent-induced tissue hyperplasia. Although further studies are needed, our results support the basic concept of stent placement in a porcine ET model.

## 5. Conclusions

Stent placement into the porcine ET was technically feasible. The luminal configuration of the placed ET stent in the pig changed according to the non-elastic nature of the cobalt–chrome alloy material and the anatomical configuration of the ET. Formation of stent-induced tissue hyperplasia was evident in the porcine ET at 4 weeks after stent placement. Various ET stent materials and designs, as well as anti-proliferative drug-coated stents, should be investigated in this animal model to optimize them for clinical trial testing. The pig is a suitable large animal model for the development of an ideal ET stent, and may also provide valuable information on long-term histopathological changes after stent placement.

**Author Contributions:** H.-Y.S., J.-H.P., and H.J.P. contributed to this work in study planning, animal experiment, data analysis, and manuscript preparation. Y.K. and W.S.K. provided data analysis and manuscript preparation with critical comments. J.M.K., D.S.R., and M.Y.K. performed the animal experiments. All authors have read and agreed to the published version of the manuscript.



**Funding:** This research was supported by a grant (2020IE0006) from the Asan Institute for Life Sciences, Asan Medical Center, Seoul, Korea.

**Institutional Review Board Statement:** This study was approved by the Institutional Animal Care and Use Committee of the Asan Institute for Life Sciences (2020-12-189) and conformed to US National Institutes of Health guidelines for humane handling of laboratory animals.

**Informed Consent Statement:** Not applicable.

**Data Availability Statement:** The data presented in this study are available on request from the corresponding author. The data are not publicly available due to ethical issues.

**Conflicts of Interest:** The authors declare no conflict of interest. The funders had no role in the design of the study; in the collection, analyses, or interpretation of data; in the writing of the manuscript; or in the decision to publish the results.

## References

- Smith, M.E.; Scoffings, D.J.; Tysome, J.R. Imaging of the Eustachian tube and its function: A systematic review. *Neuroradiology* **2016**, *58*, 543–556. [[CrossRef](#)]
- Adil, E.; Poe, D. What is the full range of medical and surgical treatments available for patients with Eustachian tube dysfunction? *Curr. Opin. Otolaryngol. Head Neck Surg.* **2014**, *22*, 8–15. [[CrossRef](#)] [[PubMed](#)]
- Bluestone, C.D. Pathogenesis of otitis media: Role of eustachian tube. *Pediatr. Infect. Dis. J.* **1996**, *15*, 281–291. [[CrossRef](#)] [[PubMed](#)]
- Wright, J.W., Jr.; Wright, J.W., 3rd. Preliminary results with use of an eustachian tube prosthesis. *Laryngoscope* **1977**, *87*, 207–214. [[CrossRef](#)] [[PubMed](#)]
- Lesinski, S.G.; Fox, J.M.; Seid, A.B.; Bratcher, G.O.; Cotton, R. Does the Silastic Eustachian Tube prosthesis improve eustachian tube function? *Laryngoscope* **1980**, *90*, 1413–1428. [[CrossRef](#)] [[PubMed](#)]
- Llewellyn, A.; Norman, G.; Harden, M.; Coatesworth, A.; Kimberling, D.; Schilder, A.; McDaid, C. Interventions for adult Eustachian tube dysfunction: A systematic review. *Health Technol. Assess.* **2014**, *18*, 1–180. [[CrossRef](#)] [[PubMed](#)]
- Kim, K.Y.; Tsauo, J.; Song, H.Y.; Park, H.J.; Kang, W.S.; Park, J.H.; Wang, Z. Fluoroscopy-guided balloon dilation in patients with Eustachian tube dysfunction. *Eur. Radiol.* **2018**, *28*, 910–919. [[CrossRef](#)]
- Song, H.Y.; Park, H.J.; Kang, W.S.; Kim, K.Y.; Park, J.H.; Yoon, S.H.; Jeon, J.Y. Fluoroscopic Balloon Dilation Using a Flexible Guide Wire to Treat Obstructive Eustachian Tube Dysfunction. *J. Vasc. Interv. Radiol.* **2019**, *30*, 1562–1566. [[CrossRef](#)]
- Pohl, F.; Schuon, R.A.; Miller, F.; Kampmann, A.; Bultmann, E.; Hartmann, C.; Lenarz, T.; Paasche, G. Stenting the Eustachian tube to treat chronic otitis media—A feasibility study in sheep. *Head Face Med.* **2018**, *14*, 8. [[CrossRef](#)]
- Ockermann, T.; Reineke, U.; Upile, T.; Ebmeyer, J.; Sudhoff, H.H. Balloon dilation eustachian tuboplasty: A feasibility study. *Otol. Neurotol.* **2010**, *31*, 1100–1103. [[CrossRef](#)]
- Kivekäs, I.; Chao, W.C.; Faquin, W.; Hollowell, M.; Silvola, J.; Rasooly, T.; Poe, D. Histopathology of balloon-dilation Eustachian tuboplasty. *Laryngoscope* **2015**, *125*, 436–441. [[CrossRef](#)] [[PubMed](#)]
- Silvola, J.; Kivekäs, I.; Poe, D.S. Balloon Dilation of the Cartilaginous Portion of the Eustachian Tube. *Otolaryngol. Head Neck Surg.* **2014**, *151*, 125–130. [[CrossRef](#)]
- Randrup, T.S.; Ovesen, T. Balloon eustachian tuboplasty: A systematic review. *Otolaryngol. Head Neck Surg.* **2015**, *152*, 383–392. [[CrossRef](#)] [[PubMed](#)]
- Ockermann, T.; Reineke, U.; Upile, T.; Ebmeyer, J.; Sudhoff, H.H. Balloon dilatation eustachian tuboplasty: A clinical study. *Laryngoscope* **2010**, *120*, 1411–1416. [[CrossRef](#)]
- Park, J.H.; Kang, W.S.; Kim, K.Y.; Kang, B.C.; Park, J.W.; Kim, M.T.; Bekheet, N.G.; Hwang, S.J.; Choi, J.; Cho, K.J.; et al. Transnasal Placement of a Balloon-Expandable Metallic Stent: Human Cadaver Study of the Eustachian Tube. *J. Vasc. Interv. Radiol.* **2018**, *29*, 1187–1193. [[CrossRef](#)] [[PubMed](#)]
- An, F.-W.; Yuan, H.; Guo, W.; Hou, Z.-H.; Cai, J.-M.; Luo, C.-C.; Yu, N.; Jiang, Q.-Q.; Cheng, W.; Liu, W.; et al. Establishment of a Large Animal Model for Eustachian Tube Functional Study in Miniature Pigs. *Anat. Rec. (Hoboken)* **2019**, *302*, 1024–1038. [[CrossRef](#)]
- Williams, B.; Taylor, B.A.; Clifton, N.; Bance, M. Balloon dilation of the Eustachian tube: A tympanometric outcomes analysis. *J. Otolaryngol. Head Neck Surg.* **2016**, *45*, 13. [[CrossRef](#)]
- Park, J.H.; Lee, J.H.; Song, H.Y.; Choi, K.D.; Ryu, M.H.; Yun, S.C.; Kim, J.H.; Kim, D.H.; Yoo, M.W.; Hwang, D.W.; et al. Over-the-wire versus through-the-scope stents for the palliation of malignant gastric outlet obstruction: A retrospective comparison study. *Eur. Radiol.* **2016**, *26*, 4249–4258. [[CrossRef](#)]
- Park, J.H.; Kim, P.H.; Shin, J.H.; Tsauo, J.; Kim, M.T.; Cho, Y.C.; Kim, J.H.; Song, H.Y. Removal of Retrievable Self-Expandable Metallic Tracheobronchial Stents: An 18-Year Experience in a Single Center. *Cardiovasc. Intervent. Radiol.* **2016**, *39*, 1611–1619. [[CrossRef](#)]
- Chew, B.H.; Denstedt, J.D. Technology insight: Novel ureteral stent materials and designs. *Nat. Clin. Pract. Urol.* **2004**, *1*, 44–48. [[CrossRef](#)]

21. Jun, E.J.; Park, J.H.; Tsauo, J.; Yang, S.G.; Kim, D.K.; Kim, K.Y.; Kim, M.T.; Yoon, S.H.; Lim, Y.J.; Song, H.Y. EW-7197, an activin-like kinase 5 inhibitor, suppresses granulation tissue after stent placement in rat esophagus. *Gastrointest. Endosc.* **2017**, *86*, 219–228. [[CrossRef](#)] [[PubMed](#)]
22. Familiari, P.; Bulajic, M.; Mutignani, M.; Lee, L.S.; Spera, G.; Spada, C.; Tringali, A.; Costamagna, G. Endoscopic removal of malfunctioning biliary self-expandable metallic stents. *Gastrointest. Endosc.* **2005**, *62*, 903–910. [[CrossRef](#)] [[PubMed](#)]
23. Faigel, D.O. Preventing biliary stent occlusion. *Gastrointest. Endosc.* **2000**, *51*, 104–107. [[CrossRef](#)]
24. Lee, H.J.; Labaki, W.; Yu, D.H.; Salwen, B.; Gilbert, C.; Schneider, A.L.; Ortiz, R.; Feller-Kopman, D.; Arias, S.; Yarmus, L. Airway stent complications: The role of follow-up bronchoscopy as a surveillance method. *J. Thorac. Dis.* **2017**, *9*, 4651–4659. [[CrossRef](#)] [[PubMed](#)]
25. Kim, K.Y.; Park, J.H.; Kim, D.H.; Tsauo, J.; Kim, M.T.; Son, W.C.; Kang, S.G.; Kim, D.H.; Song, H.Y. Sirolimus-eluting Biodegradable Poly-L-Lactic Acid Stent to Suppress Granulation Tissue Formation in the Rat Urethra. *Radiology* **2018**, *286*, 140–148. [[CrossRef](#)]
26. Park, J.H.; Kim, M.T.; Kim, K.Y.; Bakheet, N.; Kim, T.H.; Jeon, J.Y.; Jeon, J.Y.; Park, W.; Lopera, J.E.; Kim, D.H.; et al. Local Heat Treatment for Suppressing Gastroduodenal Stent-Induced Tissue Hyperplasia Using Nanofunctionalized Self-Expandable Metallic Stent in Rat Gastric Outlet Model. *ACS Biomater. Sci. Eng.* **2020**, *6*, 2450–2458. [[CrossRef](#)]
27. Park, J.H.; Park, W.; Cho, S.; Kim, K.Y.; Tsauo, J.; Yoon, S.H.; Son, W.C.; Kim, D.H.; Song, H.Y. Nanofunctionalized stent-mediated local heat treatment for the suppression of stent-induced tissue hyperplasia. *ACS Appl. Mater. Interfaces* **2018**, *10*, 29357–29366. [[CrossRef](#)]
28. Park, W.; Kim, K.Y.; Kang, J.M.; Ryu, D.S.; Kim, D.-H.; Song, H.-Y.; Kim, S.-H.; Lee, S.O.; Park, J.-H. Metallic stent mesh coated with silver nanoparticles suppresses stent-induced tissue hyperplasia and biliary sludge in the rabbit extrahepatic bile duct. *Pharmaceutics* **2020**, *12*, 563. [[CrossRef](#)]
29. Han, K.; Park, J.H.; Yang, S.G.; Lee, D.H.; Tsauo, J.; Kim, K.Y.; Kim, M.T.; Gang, S.G.; Kim, D.K.; Kim, D.H.; et al. EW-7197 eluting nano-fiber covered self-expandable metallic stent to prevent granulation tissue formation in a canine urethral model. *PLoS ONE* **2018**, *13*, e0192430. [[CrossRef](#)]
30. Park, J.H.; Kim, T.H.; Cho, Y.C.; Bakheet, N.; Lee, S.O.; Kim, S.H.; Kim, K.Y. Balloon-Expandable Biodegradable Stents Versus Self-Expandable Metallic Stents: A Comparison Study of Stent-Induced Tissue Hyperplasia in the Rat Urethra. *Cardiovasc. Interv. Radiol.* **2019**, *42*, 1343–1351. [[CrossRef](#)]
31. Varadarajulu, S.; Banerjee, S.; Barth, B.; Desilets, D.; Kaul, V.; Kethu, S.; Pedrosa, M.; Pfau, P.; Tokar, J.; Wang, A.; et al. Enteral stents. *Gastrointest. Endosc.* **2011**, *74*, 455–464. [[CrossRef](#)] [[PubMed](#)]
32. Ho, M.Y.; Chen, C.C.; Wang, C.Y.; Chang, S.H.; Hsieh, M.J.; Lee, C.H.; Wu, V.C.C.; Hsieh, I.C. The development of coronary artery stents: From bare-metal to bio-resorbable types. *Metals* **2016**, *6*, 168. [[CrossRef](#)]
33. Bowen, P.K.; Shearier, E.R.; Zhao, S.; Guillory, R.J., 2nd; Zhao, F.; Goldman, J.; Drelich, J.W. Biodegradable Metals for Cardiovascular Stents: From Clinical Concerns to Recent Zn-Alloys. *Adv. Healthc. Mater.* **2016**, *5*, 1121–1140. [[CrossRef](#)] [[PubMed](#)]
34. Mori, H.; Atmakuri, D.R.; Torii, S.; Braumann, R.; Smith, S.; Jinnouchi, H.; Gupta, A.; Harari, E.; Shkullaku, M.; Kutys, R.; et al. Very Late Pathological Responses to Cobalt-Chromium Everolimus-Eluting, Stainless Steel Sirolimus-Eluting, and Cobalt-Chromium Bare Metal Stents in Humans. *J. Am. Heart Assoc.* **2017**, *17*, e007244. [[CrossRef](#)]
35. Kereiakes, D.J.; Cox, D.A.; Hermiller, J.B.; Midei, M.G.; Bachinsky, W.B.; Nukta, E.D.; Leon, M.B.; Fink, S.; Marin, L.; Lansky, A.J. Usefulness of a cobalt chromium coronary stent alloy. *Am. J. Cardiol.* **2003**, *92*, 463–466. [[CrossRef](#)]
36. Gurr, A.; Stark, T.; Probst, G.; Dazert, S. The temporal bone of lamb and pig as an alternative in ENT-education. *Laryngorhinootologie* **2010**, *89*, 17–24. [[CrossRef](#)]